# Supplementary materials

## Temperature of artificial freshwater recharge significantly affects salinity distributions in coastal confined aquifers

Li Pu[1], Pei Xin[1, 2 #], Xiayang Yu[1], Ling Li[3], D. A. Barry[4]

[1]State Key Laboratory of Hydrology-Water Resources and Hydraulic Engineering, Hohai University, Nanjing, China

[2]Yangtze Institute for Conservation and Development, Hohai University, Nanjing, China

[3]School of Engineering, Westlake University, Hangzhou, China

[4]Laboratoire de technologie écologique (ECOL), Institut d'ingénierie de l'environnement (IIE), Faculté de l'environnement naturel, architectural et construit (ENAC), Ecole Polytechnique Fédérale de Lausanne (EPFL), Lausanne, Switzerland

[#]Corresponding author: Pei Xin, State Key Laboratory of Hydrology-Water Resources and Hydraulic Engineering, Hohai University, Nanjing, China (xinpei@hhu.edu.cn)

## 1. Numerical model

### *Governing equations*

Two-dimensional flow coupled with solute and heat transport was simulated using SUTRA-MS (Hughes & Sanford, 2004). Saturated groundwater flow in the confined aquifer is described using:

$$\rho_f S_{op} \frac{\partial p}{\partial t} + \phi\left(\frac{\partial \rho_f}{\partial C}\frac{\partial C}{\partial t} + \frac{\partial \rho_f}{\partial T}\frac{\partial T}{\partial t}\right) = -\nabla\cdot(\rho_f \overset{\mathrm{r}}{q}) + \rho^* Q^* \tag{1a}$$

$$\overset{\mathrm{r}}{q} = -\left(\frac{k}{\mu}\right)\cdot(\nabla p - \rho_f g) \tag{1b}$$

$$S_{op} = (1-\phi)\alpha + \phi\beta \tag{1c}$$

where $\phi$ is the soil porosity [-], $p$ is the fluid pressure [M/LT$^2$], $t$ is the time [T], $k$ is the intrinsic permeability [L$^2$], $\mu$ is the fluid viscosity [M/LT], $\rho_f$ is the fluid density [M/L$^3$], $g$ is the magnitude of the gravitational acceleration [L/T$^2$], $Q^*$ is the fluid source [T$^{-1}$], $\rho^*$ is the density of the fluid source [M/L$^3$], $C$ is the salt concentration [-], $T$ is the temperature [°C], $\vec{q}$ is the Darcy velocity [L/T], $S_{op}$ is the specific pressure storativity [M/LT$^2$]$^{-1}$, $\alpha$ is the compressibility of the porous matrix [M/LT$^2$]$^{-1}$ and $\beta$ is the compressibility of the fluid [M/LT$^2$]$^{-1}$.

In Equation 1, $\rho_f$ (kg/m$^3$) is given as (van Lopik et al., 2015):

$$\rho_f = \rho_0 + \beta_C C + \beta_T T \tag{2}$$

where $\rho_0$ is the benchmark fluid density (considered here as the fluid density of freshwater at 0°C). In (2), $\beta_C$ and $\beta_T$ are the coefficients of volumetric expansion for salinity and temperature, respectively. In this study, $\rho_f = 1002 + 0.7705C - 0.2205T$. The fluid viscosity, $\mu$ (kg/m/s), is given by (Hughes & Sanford, 2004):

$$\mu = 239.4\times10^{\frac{248.37}{T+133.15}-7} \tag{3}$$

Salt and heat transport in the confined aquifer are modeled using (Hughes & Sanford, 2004):

**Salt transport**

$$\frac{\partial\left(\phi\rho_f C\right)}{\partial t} = -\nabla\cdot\left(\rho_f \vec{q}C\right)+\nabla\cdot\left(\phi\rho_f \mathbf{D}_S\nabla C\right)+\rho^* Q^* C^* \tag{4}$$

**Heat transport**

$$\frac{\partial\left[\phi\rho_f c_f +\left(1-\phi\right)\rho_s c_s\right]T}{\partial t} = -\nabla\cdot\left(\rho_f c_f \vec{q}T\right)+\nabla\cdot\left(\rho_f c_f D_T\nabla T\right)+c_f\rho^* Q^* T^* \tag{5a}$$

$$D_T = \frac{\phi\lambda_f +\left(1-\phi\right)\lambda_s}{\rho_f c_f} \tag{5b}$$

where $\mathbf{D}_S$ is the diffusion coefficient tensor. It is composed of the mechanical dispersion tensor ($\underline{\mathbf{D}}$) and molecular diffusivity $D_M$ [L$^2$/T], i.e., $\mathbf{D}_S = \underline{\mathbf{D}} + D_M\mathbf{I}$ in which $\mathbf{I}$ is the identity tensor, $\rho_s$ is the density of the solid matrix [M/L$^3$], $c_s$ is the solid matrix specific heat [E/M°C], $c_f$ is the fluid specific heat [E/M°C], $D_T$ is the effective thermal diffusivity [L$^2$/T], $\lambda_f$ is the fluid thermal conductivity [E/TL°C], $\lambda_s$ is the solid thermal conductivity [E/TL°C], $C^*$ [-] and $T^*$ [°C] are the salt concentration and temperature of the fluid source, respectively. Note that $\phi\rho_f c_f +\left(1-\phi\right)\rho_s c_s$ in Eq. (5a) gives the bulk heat capacity and $\phi\lambda_f +\left(1-\phi\right)\lambda_s$ in Eq. (5b) gives thermal conductivity of the saturated soil.

In the numerical model, the inland boundary was given by a specified water flux and a fixed temperature of 25°C. The salinity was set to 0 ppt. For the seaward boundary, a hydrostatic pressure distribution corresponding to the given seawater level was imposed (salinity at 35 ppt). The temperature was also fixed at 25°C. In SURTA-MS, zero salinity and temperature gradients are specified at nodes with outflow (from the aquifer) (Hughes &

Sanford, 2004). In this way, the simulated salinity and temperature values could differ from those specified for this boundary condition. The recharged water was considered as a source term with fixed temperature and salinity (0 ppt).

## 2. Locations of thermometers installed in the laboratory flume

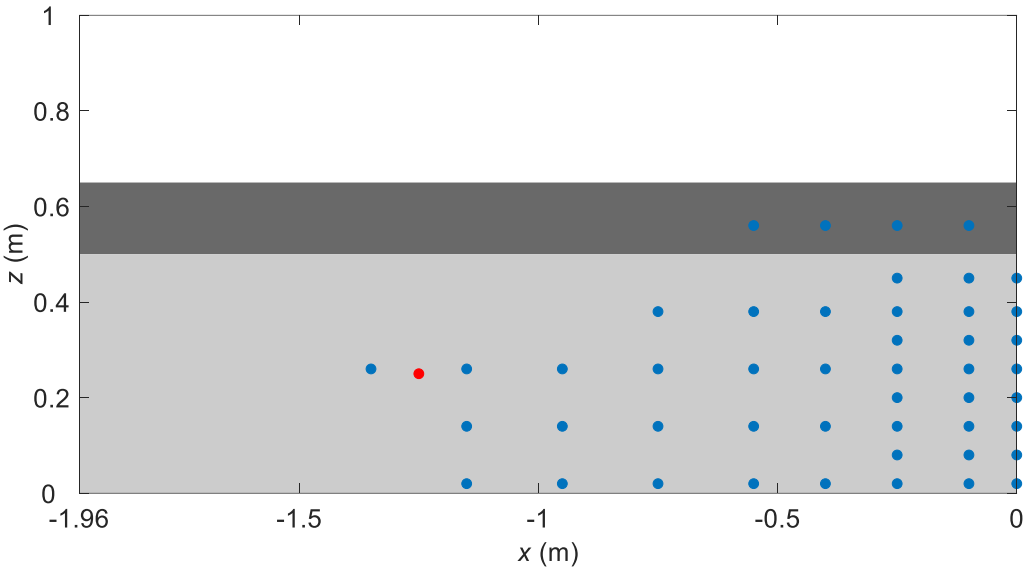


Figure S1. Locations of thermometers (blue dots) installed in the laboratory flume. The dark grey zone indicates the clay layer and the light grey zone indicates the sand layer. The red dot indicates the injection point.

**3. Additional results related to the laboratory-scale aquifer**

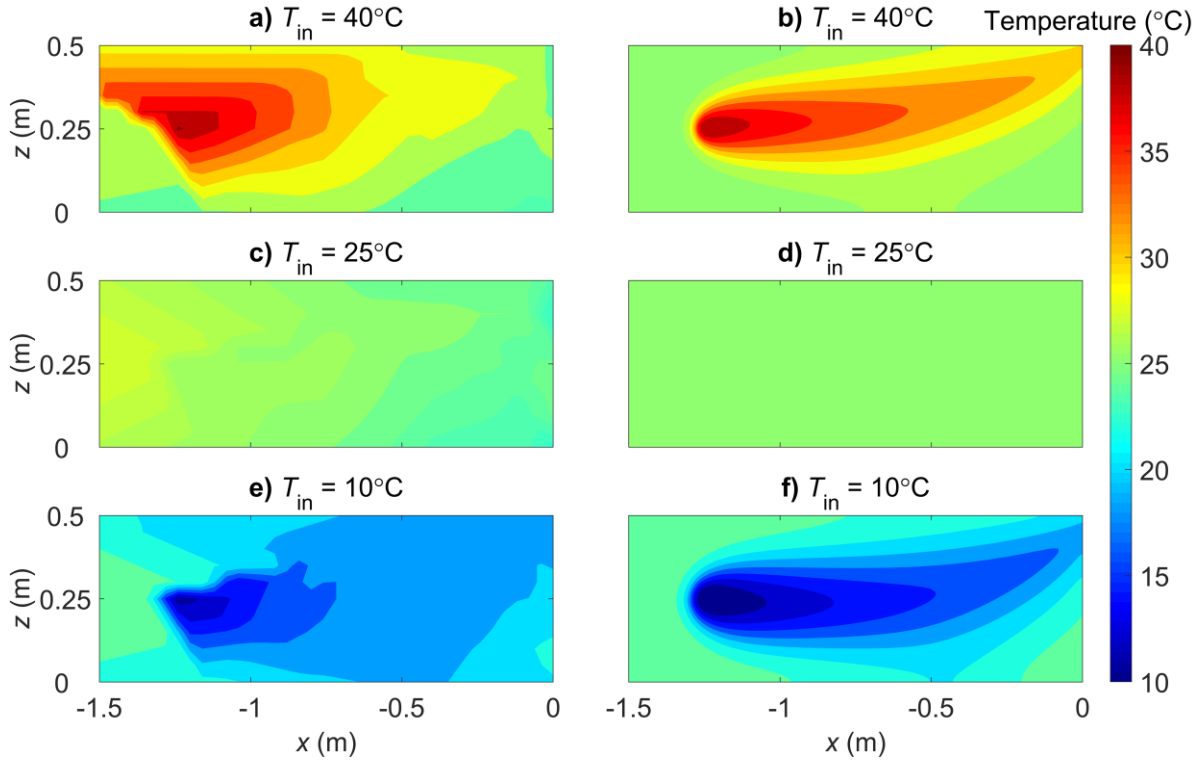


Figure S2. Comparison of experimental (a, c, e) and simulated (b, d, f) temperature distributions.

While heat dissipation led to differences between the measured and simulated temperature distributions shown in Figure S2, the patterns in the aquifer agreed.

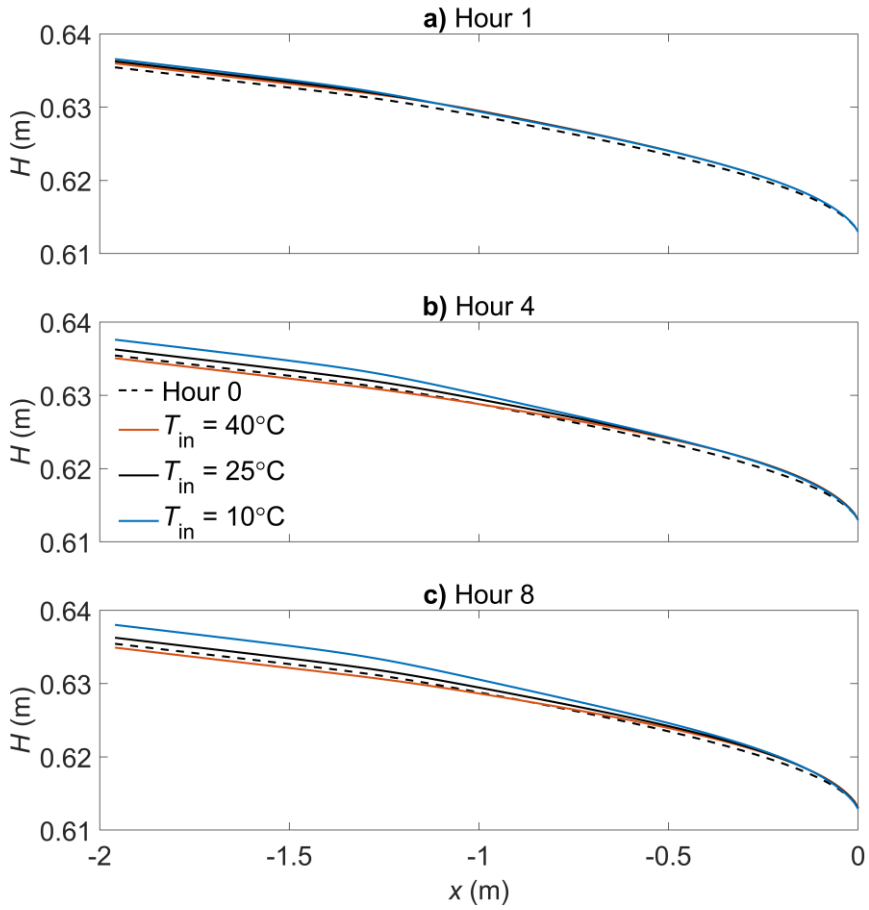


Figure S3. Watertables in the aquifers at different times after the freshwater injection. $T_{in}$ indicates the temperatures of the injected water. For comparison, the watertable prior to the injection (Hour 0) is also given.

It can be seen in Figure S3 that with hot (40°C) water injection, the watertable in the inland area ($x$ from -2 to -1 m) first rose up (Figure S3a) but afterwards dropped down (Figure S3b, c).

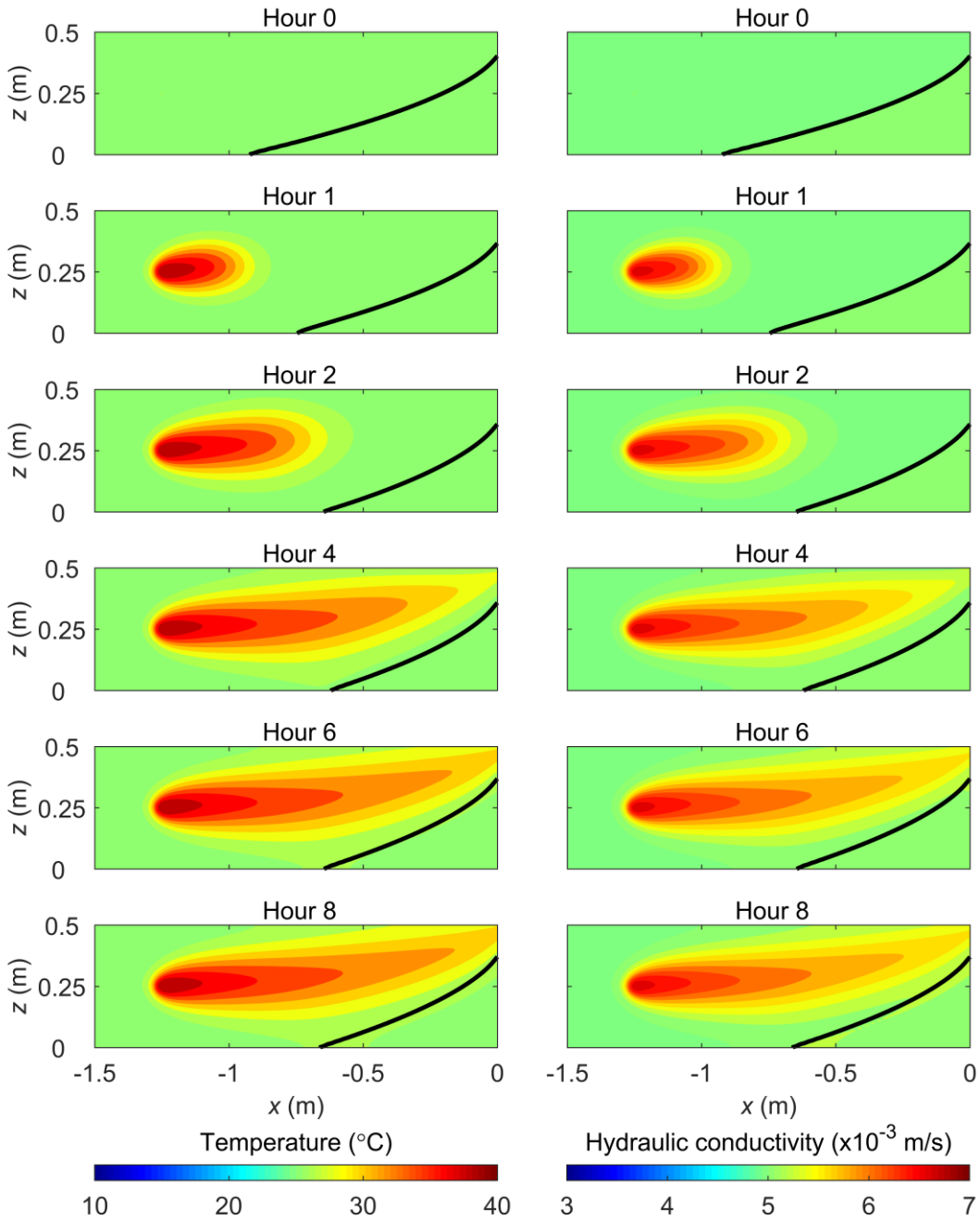


Figure S4. Results for injected water temperature set to 40°C. Temperature distributions (left panels) and hydraulic conductivity distributions (right panels) at different times after the freshwater injection. The black lines show the simulated interfaces between freshwater and seawater.

It can be seen in Figure S4 that the injected hot water (locally) heated the aquifer and increased the hydraulic conductivity.

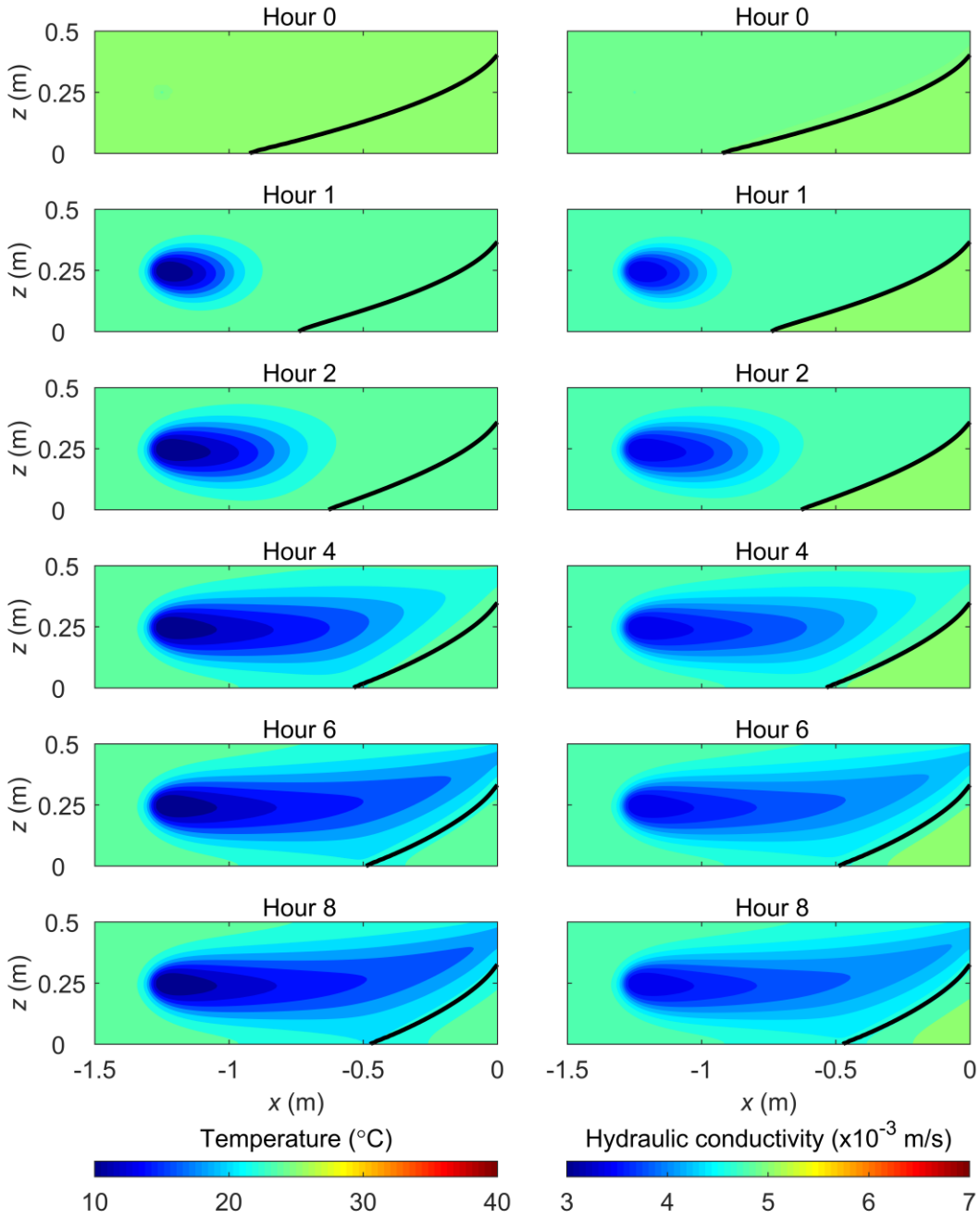


Figure S5. Results for injected water temperature set to 10°C. Temperature distributions (left panels) and hydraulic conductivity distributions (right panels) at different times after the freshwater injection. The black lines show the simulated interfaces between freshwater and seawater.

Figure S5 shows that the injected cold water (locally) cooled down the aquifer and decreased the hydraulic conductivity.

## 4. Results related to the large-scale and confined aquifer

A two-dimensional (cross-shore section) confined aquifer between two impermeable layers was considered. The rectangular domain was 400 m in length and 100 m in height. The top and bottom boundaries were set to no flow. A fixed per-unit-width flux ($6.6 \times 10^{-5}$ $m^3/m/s$) was given on the left (landward) side (salinity was set to 0 ppt). A fixed seawater level (100 m) was set along the right (seaward) side (salinity was set to 35 ppt). For each case, after the simulation reached the steady state, freshwater was injected at $x$ = -250 m, $z$ = 50 m at a rate of $4 \times 10^{-5}$ $m^3/m/s$.

Table S1. Parameter values used for the large-scale and homogenous confined aquifer simulations.

| Symbol | Parameter | Value | Unit |
|---|---|---|---|
| $\phi$ | porosity | 0.35 | - |
| $k$ | intrinsic permeability | $10^{-11}$ | $m^2$ |
| $\alpha_L$ | longitudinal dispersivity | 1 | m |
| $\alpha_T$ | transverse dispersivity | 0.1 | m |
| $c_f$ | fluid specific heat | 4182 | J/kg/°C |
| $c_s$ | solid matrix specific heat | 840 | J/kg/°C |
| $\lambda_f$ | fluid thermal conductivity | 0.6 | J/m/°C/s |
| $\lambda_s$ | solid thermal conductivity | 3.5 | J/m/°C/s |
| $D_M$ | molecular diffusivity | $10^{-9}$ | $m^2/s$ |
| $\alpha$ | compressibility of the solid matrix | $10^{-7}$ | $Pa^{-1}$ |
| $\beta$ | compressibility of the fluid | $4.47 \times 10^{-10}$ | $Pa^{-1}$ |

Both homogenous and heterogeneous aquifers were considered. For the homogenous aquifer, the parameter values used are listed in Table S1. For the heterogeneous aquifer, the approach of Bellin and Rubin (1996) was used to generate a heterogeneous permeability field. The distribution of permeability was lognormal and characterized by a mean $E[\ln(k)]$ = -25.32 and variance $\sigma^2[\ln(k)] = 0.4$. The spatially correlated structure was described by an

exponential-decay covariance function with the horizontal and vertical correlation lengths being $\lambda_x$ = 1 m and $\lambda_z$ = 0.1 m, respectively (Figure S9). Other parameters were the same as those for the homogenous aquifer. For each aquifer type, three cases with different temperatures of injected freshwater were considered ($T_{in}$ = 40, 25 and 10°C).

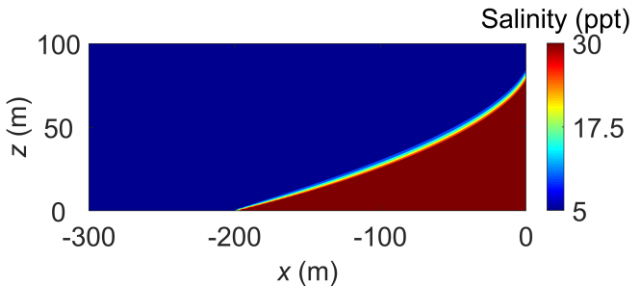


Figure S6. Steady state salinity distribution in the large-scale, homogenous confined aquifer prior to the freshwater injection.

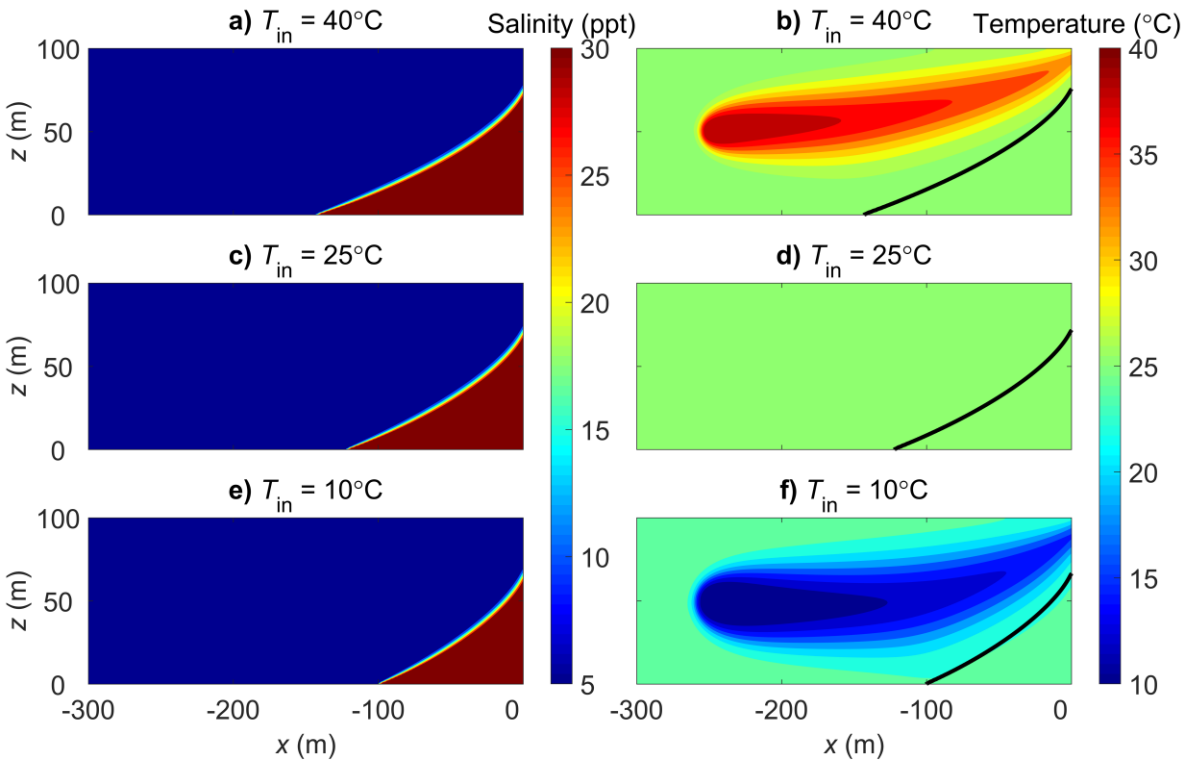


Figure S7. Steady state salinity distributions (left panels) and temperature distributions (right panels) in the large-scale, homogenous confined aquifers. The black lines show the simulated interfaces between freshwater and seawater. $T_{in}$ indicates the temperature of the injected water.

It is evident from Figure S7 that the hot freshwater recharge induced a larger saltwater wedge, consistent with the results at the laboratory scale.

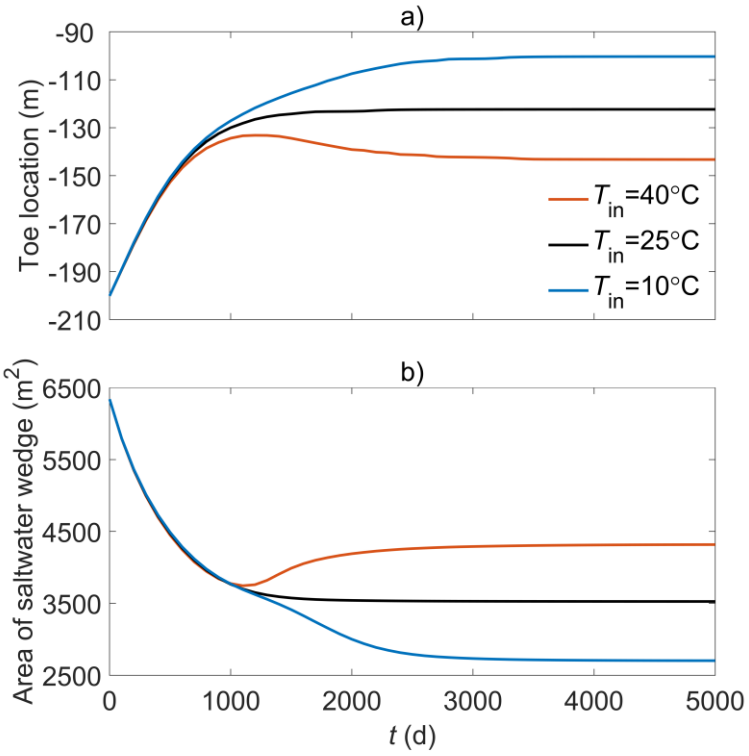


Figure S8. Variations of the toe locations (a) and areas of saltwater wedge (b) in the large-scale, homogenous confined aquifers after the freshwater injection. $T_{in}$ indicates the temperature of the injected water.

Except for larger response time, the results in Figure S8 are consistent with those at the laboratory scale: (1) the response of the salinity distribution to the cold-water injection was prolonged and (2) hot water injection incurred an overshoot phenomenon. The salt wedge retreated seaward first but intruded back until it reached steady state.

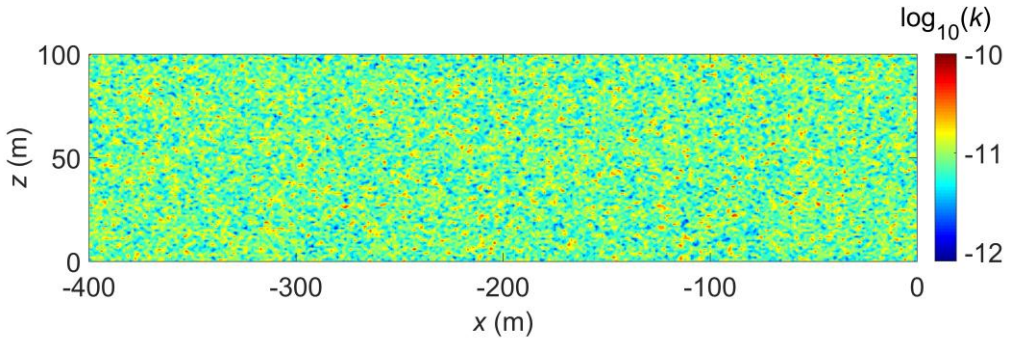


Figure S9. Distribution of the soil permeability (unit: m$^2$) of a large-scale, heterogeneous confined aquifer.

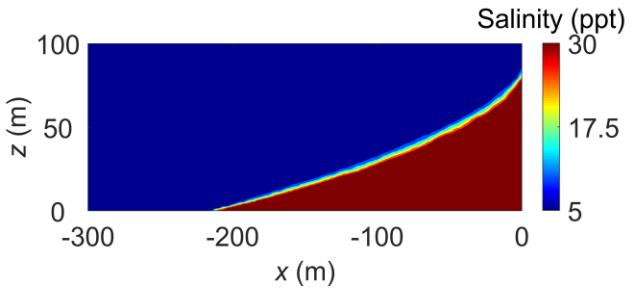


Figure S10. Steady state salinity distribution in the large-scale, heterogeneous confined aquifer prior to the freshwater injection.

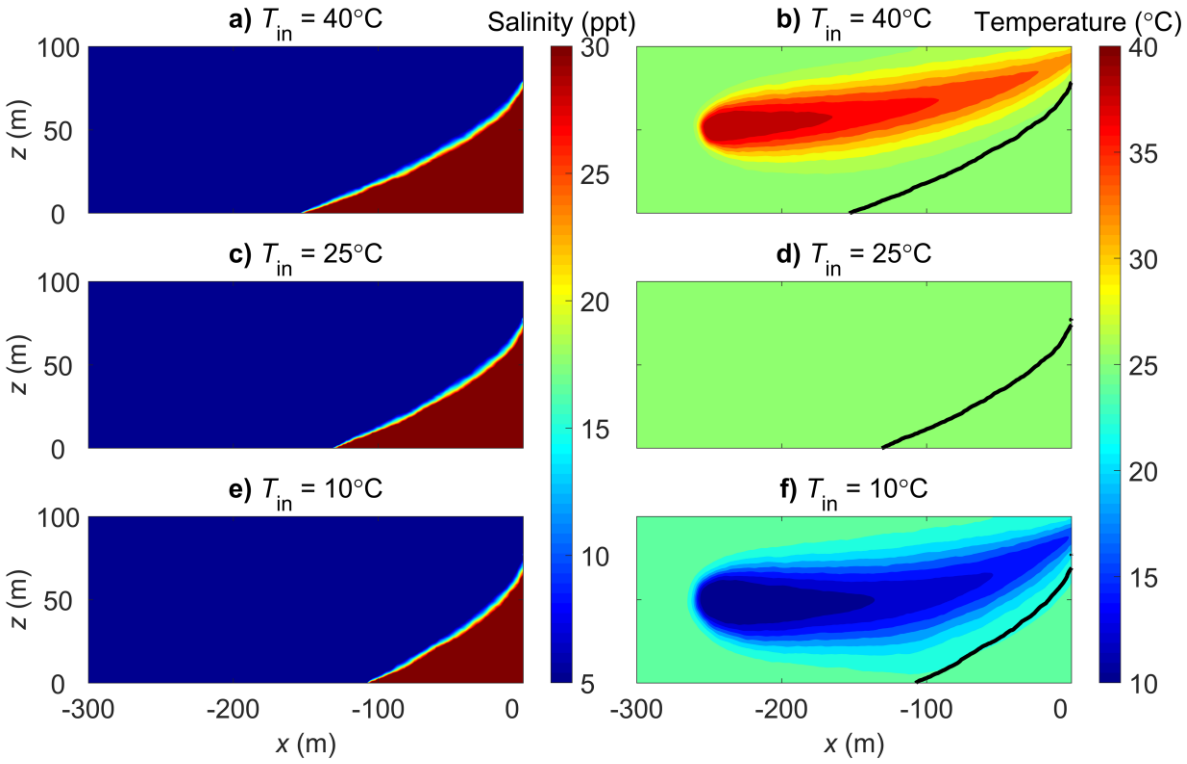


Figure S11. Salinity distributions (left panels) and temperature distributions (right panels) in the large-scale, heterogeneous confined aquifers. The black lines show the simulated interfaces between freshwater and seawater. $T_{in}$ indicates the temperature of the injected water.

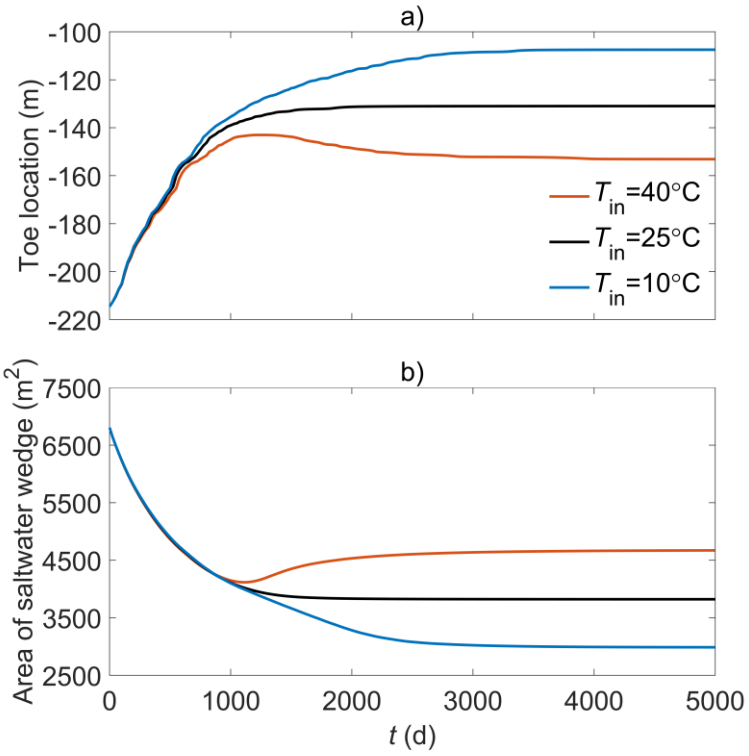


Figure S12. Variations of the toe locations (a) and areas of saltwater wedge (b) in the large-scale, heterogeneous confined aquifers after the freshwater injection. $T_{in}$ indicates the temperature of the injected water.